

Casimir-Polder shift of ground-state hyperfine Zeeman sub-levels of hydrogen isotopes in a micron-sized metallic cavity at finite temperature

Davide Iacobacci^{1,2}, Giuseppe Bimonte^{1,2}, and Thorsten Emig³

¹*Dipartimento di Fisica E. Pancini, Università di Napoli Federico II,
Complesso Universitario di Monte S. Angelo, Via Cintia, I-80126 Napoli, Italy*

²*INFN Sezione di Napoli, I-80126 Napoli, Italy and*

³*Laboratoire de Physique Théorique et Modèles Statistiques,
CNRS UMR 8626, Université Paris-Saclay, 91405 Orsay cedex, France**

The frequencies of transitions between hyperfine levels of ground-state atoms can be measured with exquisite precision using magnetic-resonance techniques. This makes hyperfine transitions ideal probes of QED effects originating from the interaction of atoms with the quantized electromagnetic field. One of the most remarkable effects predicted by QED is the Casimir-Polder shift experienced by the energy levels of atoms placed near one or more dielectric objects. Here we compute the Casimir-Polder shift and the width of hyperfine transitions between ground-state Zeeman sub-levels of an hydrogen atom placed in a micron-sized metallic cavity, over a range of temperatures extending from cryogenic temperatures to room temperature. Results are presented also for deuterium and tritium. We predict shifts of the hyperfine transitions frequencies of a few tens of Hz that might be measurable with present-day magnetic resonance apparatus.

PACS numbers: 12.20.-m, 03.70.+k, 42.25.Fx

I. INTRODUCTION

A fundamental problem in atomic physics is the interaction of atoms with radiation fields. The atom's coupling with quantum fluctuations of the electromagnetic (em) field causes the spontaneous decay of excited states, and leads to the famous Lamb shift. Studies carried out over the past seventy years or so revealed that atomic level positions are corrected by two further effects, that were not considered in the original Lamb shift. On one hand, it was realized that at finite temperature, besides virtual photons that are responsible of the Lamb shift, real photons give rise to a temperature-dependent correction of atomic levels [1–4]. A different interesting situation is that of an atom in a confined geometry. Since the presence of material boundaries modifies the spectrum of the modes of the em field, the lifetimes and energies of the atom's excited states are shifted [5, 6]. Even though the ultimate explanation of the latter phenomena is basically the same as the Lamb shift, i.e. coupling of the atom with the modes of the em field, the term "Lamb shift" usually refers to the shift of energy levels experienced by an atom in free space (at zero temperature). The additional correction to the energy levels resulting from the presence of one or more material surfaces (possibly at finite temperature) is referred to as Casimir-Polder (CP) shift (for a recent review of the CP interaction, see the book [7] and references therein).

The observation of shifts of atomic energy levels induced by thermal radiation and/or by the CP interac-

tion is difficult, because the theoretically predicted magnitude of the shifts is extremely small. Over the past forty years, however, several experiments succeeded in observing these tiny effects, using high-precision laser spectroscopy techniques. In [8] the shift of Rydberg energy levels of Rb atoms induced by black-body radiation was measured in free space. The reported fractional shifts of $\sim 2 \times 10^{-12}$ were found to be consistent with theoretical expectations. A more recent experiment [9] observed the shift of Rydberg energy levels of Rb atoms confined between two parallel metal plates. In this experiment the plate distance, of the order of a mm, was tuned over the wavelength of the relevant Rydberg transitions. At resonance, level shifts of the order of 100 Hz were observed, for a range of temperatures extending from room temperature down to 4 K, again in good agreement with theory. A spectroscopic observation of the CP shift of the levels of Rydberg Na atoms in a non-resonant micron-sized cavity was reported in [10]. In the regime probed in this experiment, the CP interaction was observed in the non-retarded limit, where temperature effects are negligible.

In this paper, we compute the thermal CP shift of the transition frequencies among ground-state hyperfine Zeeman sub-levels of a hydrogen atom, placed in a micron-sized metallic cavity at finite temperature. Besides hydrogen, we shall also consider its isotopes deuterium (D) and tritium (T). The present work is a follow-up of the companion paper [11], where we investigated the influence of the CP interaction on the transition rates between hyperfine ground-state sub-levels of D atoms, passing between two closely spaced Au mirrors at room temperature. In that paper, it was shown that the space between the mirrors is filled with a broad non-Planckian spectrum of em noise, mainly consisting of thermal fluctuations of the magnetic field. The energy density of these em fields is enormous: in [11] it was estimated that at the center

*Electronic address: davide.iacobacci@unina.it,
giuseppe.bimonte@na.infn.it, thorsten.emig@universite-paris-saclay.fr

of a 2 μm Au cavity at room temperature, this density is about 700 times larger than the energy density of a black-body at the same temperature. The existence of such a strong fluctuating magnetic field leads one to expect that the properties of the hyperfine sub-levels of an atom placed inside a cavity might be strongly affected, via coupling with the atom's magnetic moment. This expectation was indeed confirmed by the computations presented in [11], where it was found that the transition rates between hyperfine sub-levels of D atoms placed at the center of a 2 μm Au cavity at room temperature increase by approximately 15 orders of magnitude compared to the corresponding rates in a large black-body at the same temperature.

In [11] we investigated the *absorptive* component of the CP atom-wall interaction, which determines the transition rates among the hyperfine atomic levels. In the present work we consider the *dispersive* component of the interaction to compute the frequency shift and width of the hyperfine transitions of H atoms. A preliminary investigation of this problem was sketched in [12], where the shift of the energy of the 5s $|F, m_F\rangle = |1, -1\rangle$ ground-state hyperfine level of a Rb atom placed near a single metallic plate was estimated on the basis of a simplified two-level model of the atom. In this paper the problem is studied on the basis of a realistic model of the atom, which takes into account all its excited states.

The paper is organized as follows. In Sec. II we review the perturbative theory of Wylie and Sipe [5] which can be used to compute the CP interaction of an atom with a material wall at finite temperature. In Sec. III we review some basic facts on the hyperfine structure of atomic spectra. These notions are well-known to atomic physicists. They are reviewed here for the benefit of readers working in the field of Casimir physics, who may not be fully familiar with the properties of hyperfine states of atoms. In Sec. IV we compute the shift of hyperfine transitions induced by black-body radiation in free-space, while in Sec. V we consider the case of an atom placed inside a cavity at finite temperature. In Sec. VI we present our conclusions. Finally, in the Appendices we derive the formulae for the matrix elements of the magnetic and electric dipole operators that are needed in the computation of the shift of hyperfine transitions, and we provide the explicit expression of the Green function of the electromagnetic field inside a dielectric cavity. Gaussian electromagnetic units are used throughout.

II. THEORY

In this Section, we shall briefly review the basic theory that allows to compute the shifts and the widths of the spectral lines of an atom placed at the point \mathbf{r}_0 near one or more material surfaces. The surfaces are assumed to be in thermal equilibrium with the environment at temperature T .

By working in the dipole approximation and using

second-order perturbation theory, Wylie and Sipe [5] showed that the shift of the energy of the state $|a\rangle$ of an atom exposed to thermal radiation can be decomposed as the sum of a dynamic Stark effect $\delta\mathcal{F}_a^{(E)}$ induced by the atom's coupling to the thermal and quantum fluctuations of the electric field, plus a dynamic Zeeman effect $\delta\mathcal{F}_a^{(H)}$ induced by the atom's coupling to the thermal and quantum fluctuations of the magnetic field,

$$\delta\mathcal{F}_a = \delta\mathcal{F}_a^{(E)} + \delta\mathcal{F}_a^{(H)}, \quad (1)$$

where

$$\delta\mathcal{F}_a^{(E)} = -\frac{1}{\pi} \sum_b d_i^{ab} d_j^{ba} \mathcal{P} \int_{-\infty}^{\infty} \frac{d\omega \text{Im}[\mathcal{E}_{ij}(\mathbf{r}_0, \mathbf{r}_0; \omega)]}{(\omega + \omega_{ba})(1 - e^{-\hbar\omega/k_B T})}, \quad (2)$$

$$\delta\mathcal{F}_a^{(H)} = -\frac{1}{\pi} \sum_b \mu_i^{ab} \mu_j^{ba} \mathcal{P} \int_{-\infty}^{\infty} \frac{d\omega \text{Im}[\mathcal{H}_{ij}(\mathbf{r}_0, \mathbf{r}_0; \omega)]}{(\omega + \omega_{ba})(1 - e^{-\hbar\omega/k_B T})} \quad (3)$$

In the above Equations, the symbol \mathcal{P} denotes the principal value, latin indices $i, j = 1, 2, 3$ denote spatial directions, with repeated indices summed over, and the symbol \sum denotes a sum over discrete states, as well as in integral over continuum states. Moreover we define the transition frequency

$$\omega_{ba} = (E_b - E_a)/\hbar, \quad (4)$$

where E_a is the unperturbed energy of state a , $d_i^{ab} = \langle a | \hat{d}_i | b \rangle$ and $\mu_i^{ab} = \langle a | \hat{\mu}_i | b \rangle$ are, respectively, the matrix elements of the atom's electric and magnetic dipole moment operators, and $\mathcal{E}_{ij}(\mathbf{r}, \mathbf{r}'; \omega)$ and $\mathcal{H}_{ij}(\mathbf{r}, \mathbf{r}'; \omega)$ denote, respectively, the Fourier transformed [28] classical Green tensors of the electric and magnetic fields.

In investigations of the CP interaction of atoms with material surfaces the contribution of the dynamic Zeeman effect $\delta\mathcal{F}_a^{(H)}$ is usually negligible, and the entire interaction originates from the dynamic Stark effect. Contrary, in the problem studied in this paper, i.e. the CP shift of the transition frequencies among hyperfine Zeeman sub-levels of ground state atoms, the opposite true. We shall find that the dominant role is indeed played by the dynamic Zeeman effect.

As stated already, Eq. (3) is derived on the basis of second-order perturbation theory. An elegant non-perturbative computation of the energy shifts, based on the solution of the coupled dynamics of the *macroscopic* quantized em field and the atomic system, is offered in [13] (see also the book [7]). We note that the non-perturbative result of [13] correctly reproduces Eq. (3) in the weak-coupling limit.

In their paper, Wylie and Sipe actually used Eq. (3) for $T = 0$, and they refer to $\delta\mathcal{F}_a$ as the atom's 'energy' shift, which is indeed correct at zero temperature. The careful analysis carried out by Barton [14] shows that for finite temperature T , the quantity $\delta\mathcal{F}_a$ actually represents the shift of the Helmholtz free-energy of the *constrained* equilibrium thermodynamic system formed by the atom together with the quantized em field. Here, the atom's state

label a plays the same role as a macroscopically controlled variable in ordinary thermodynamics. For brevity, in what follows we shall keep referring to $\delta\mathcal{F}_a$ as the energy-shift of state a . According to Ref. [14] the shifts $\delta\nu_{aa'}$ of the atom's transition frequencies $\nu_{aa'} = (E_a - E_{a'})/h$ (we assume $E_a > E_{a'}$ so that $\nu_{aa'}$ is defined to be positive) are calculable as the differences between the coupling-induced shifts of the free energies of the corresponding states,

$$\delta\nu_{aa'} = (\delta\mathcal{F}_a - \delta\mathcal{F}_{a'})/h, \quad (E_a > E_{a'}). \quad (5)$$

In view of our sign convention for the frequencies $\nu_{aa'}$, a positive $\delta\nu_{aa'} > 0$ indicates that the transition frequency is shifted towards larger frequencies, while a negative $\delta\nu_{aa'} < 0$ indicates a shift towards lower frequencies. We see from Eq. (1) that similarly to the energy-shift, the frequency shift $\delta\nu_{aa'}$ can be also expressed as the sum of the dynamic Stark shift $\delta\nu_{aa'}^{(E)}$ and the dynamic Zeeman shift $\delta\nu_{aa'}^{(H)}$,

$$\delta\nu_{aa'} = \delta\nu_{aa'}^{(E)} + \delta\nu_{aa'}^{(H)}, \quad (6)$$

where

$$\delta\nu_{aa'}^{(E)} = (\delta\mathcal{F}_a^{(E)} - \delta\mathcal{F}_{a'}^{(E)})/h, \quad (7)$$

$$\delta\nu_{aa'}^{(H)} = (\delta\mathcal{F}_a^{(H)} - \delta\mathcal{F}_{a'}^{(H)})/h. \quad (8)$$

Using first-order perturbation theory, Wylie and Sipe obtained the following expression for the transition probabilities A_{ba} of the allowed dipole transitions from state a to state b ,

$$A_{ba} = \frac{2/\hbar}{1 - e^{-\hbar\omega_{ab}/k_B T}} \left\{ d_i^{ab} d_j^{ba} \text{Im}[\mathcal{E}_{ij}(\mathbf{r}_0, \mathbf{r}_0, \omega_{ab})] + \mu_i^{ab} \mu_j^{ba} \text{Im}[\mathcal{H}_{ij}(\mathbf{r}_0, \mathbf{r}_0, \omega_{ab})] \right\}. \quad (9)$$

By summing the transition rate over all final states, one obtains the total depopulation rate Γ_a ,

$$\Gamma_a = \sum_{b \neq a} A_{ba}. \quad (10)$$

As it is well known [15], the half-width $\Delta\omega_{1/2}$ of the spectral line corresponding to transitions between states a and b is the sum of the depopulation rates of the states a and b ,

$$\Delta\omega_{1/2} = \Gamma_b + \Gamma_a. \quad (11)$$

We note that by virtue of the reciprocity relations satisfied by the Green tensors $\mathcal{E}_{ij}(\mathbf{r}, \mathbf{r}'; \omega) = \mathcal{E}_{ji}(\mathbf{r}', \mathbf{r}; \omega)$ and $\mathcal{H}_{ij}(\mathbf{r}, \mathbf{r}'; \omega) = \mathcal{H}_{ji}(\mathbf{r}', \mathbf{r}; \omega)$ [7], the products of the dipole moments in Eqs. (3) and (9) can be actually replaced by their symmetrized products,

$$\begin{aligned} d_i^{ab} d_j^{ba}|_{\text{sym}} &\equiv \frac{d_i^{ab} d_j^{ki} + d_j^{ab} d_i^{ba}}{2}, \\ \mu_i^{ab} \mu_j^{ba}|_{\text{sym}} &\equiv \frac{\mu_i^{ab} \mu_j^{ba} + \mu_j^{ab} \mu_i^{ba}}{2}. \end{aligned} \quad (12)$$

Eqs. (3) and (9) provide the general framework for studying the shifts and the radiative widths of the spectral lines of an atom which interacts with the radiation field surrounding one or more dielectric bodies, in thermal equilibrium with the environment. In the following subsection, we shall study first the simple situation of an atom exposed to black-body radiation in free-space, while in subsection B we shall consider the more complicated case of an atom placed inside a cavity.

A. An atom in free space

The shifts and the radiative widths of the spectral lines of an atom, exposed to black-body radiation in free-space, can be computed by substituting into Eqs. (3) and (9) the free-space Green tensors $\mathcal{E}_{ij}^{(0)}(\mathbf{r}, \mathbf{r}'; \omega)$ and $\mathcal{H}_{ij}^{(0)}(\mathbf{r}, \mathbf{r}'; \omega)$. The expressions of the latter Green tensors are provided in Appendix B. It can be seen from Eq. (B3) that in the coincidence limit $\mathbf{r} = \mathbf{r}' = \mathbf{r}_0$ the real parts of the free-space Green tensors diverge, while their imaginary parts attain the finite limit

$$\text{Im}[\mathcal{E}_{ij}^{(0)}(\mathbf{r}_0, \mathbf{r}_0; \omega)] = \text{Im}[\mathcal{H}_{ij}^{(0)}(\mathbf{r}_0, \mathbf{r}_0; \omega)] = \frac{2\omega^3}{3c^3} \delta_{ij}. \quad (13)$$

When the latter formula is substituted back into Eq. (3) it is not hard to verify that the energy-shift $\delta\mathcal{F}_a^{(0)}$ can be decomposed into the sum of two terms,

$$\delta\mathcal{F}_a^{(0;\text{bare})} = \delta\mathcal{F}_a^{(0;\text{zp})} + \delta\mathcal{F}_a^{(0;\text{th})}, \quad (14)$$

where we have defined the zero-point contribution

$$\delta\mathcal{F}_a^{(0;\text{zp})} = -\frac{2}{3\pi c^3} \sum_b (d_i^{ab} d_i^{ba} + \mu_i^{ab} \mu_i^{ba}) \text{P} \int_0^\infty \frac{d\omega \omega^3}{(\omega_{ba} + \omega)}. \quad (15)$$

and the thermal shift

$$\delta\mathcal{F}_a^{(0;\text{th})}(T) = \delta\mathcal{F}_a^{(0;\text{th}|E)}(T) + \delta\mathcal{F}_a^{(0;\text{th}|H)}(T), \quad (16)$$

with

$$\begin{aligned} \delta\mathcal{F}_a^{(0;\text{th}|E)}(T) &= -\frac{2\hbar}{3\pi c^3} \text{P} \int_0^\infty d\omega \frac{\omega^3 \alpha_{ii}^{(a)}(\omega)}{(e^{\hbar\omega/k_B T} - 1)}, \\ \delta\mathcal{F}_a^{(0;\text{th}|H)}(T) &= -\frac{2\hbar}{3\pi c^3} \text{P} \int_0^\infty d\omega \frac{\omega^3 \beta_{ii}^{(a)}(\omega)}{(e^{\hbar\omega/k_B T} - 1)}. \end{aligned} \quad (17)$$

Here, $\alpha_{ij}^{(a)}(\omega)$ and $\beta_{ij}^{(a)}(\omega)$ denote, respectively, the electric and magnetic polarizabilities of the atom in the state a [18],

$$\alpha_{ij}^{(a)}(\omega) = \frac{1}{\hbar} \sum_{b \neq a} \left(\frac{d_i^{ab} d_j^{ba}}{\omega_{ba} - \omega} + \frac{d_j^{ab} d_i^{ba}}{\omega_{ba} + \omega} \right), \quad (18)$$

$$\beta_{ij}^{(a)}(\omega) = \frac{1}{\hbar} \sum_{b \neq a} \left(\frac{\mu_i^{ab} \mu_j^{ba}}{\omega_{ba} - \omega} + \frac{\mu_j^{ab} \mu_i^{ba}}{\omega_{ba} + \omega} \right). \quad (19)$$

We note that the contribution $\delta\mathcal{F}_a^{(0;\text{zp})}$ in Eq. (15) is expressed by an UV-divergent integral over frequency, which is independent of temperature. This allows to interpret $\delta\mathcal{F}_a^{(0;\text{zp})}$ as representing the formally divergent shift of the atom's energy engendered by the atom's coupling to vacuum fluctuations of the em field, i.e. its Lamb shift. Clearly, the non-relativistic theory behind Eq. (3) cannot properly account for this effect, whose computation requires consideration of the full relativistic quantum theory. One can thus neglect $\delta\mathcal{F}_a^{(0;\text{zp})}$, and just retain the second term $\delta\mathcal{F}_a^{(0;\text{th})}(T)$ in Eq. (14), which provides the temperature-dependent energy shift of an atom interacting with a thermal bath,

$$\delta\mathcal{F}_a^{(0)} = \delta\mathcal{F}_a^{(0;\text{th})}(T). \quad (20)$$

An Equation equivalent to Eq. (20) was indeed derived in Ref. [4], where it was used to compute the dynamic Stark shifts $\delta\mathcal{F}_a^{(0;\text{th}|E)}(T)$ of Rydberg states of hydrogen, helium and alkali-metal atoms induced by black-body radiation. Following this reference, we recast $\delta\mathcal{F}_a^{(0;\text{th}|E)}(T)$ and $\delta\mathcal{F}_a^{(0;\text{th}|H)}(T)$ in the form

$$\begin{aligned} \delta\mathcal{F}_a^{(0;\text{th}|E)} &= \frac{2}{3\pi c^3} \left(\frac{k_B T}{\hbar} \right)^3 \sum_{b \neq a} \sum_i |d_i^{ab}|^2 F \left(\frac{E_a - E_b}{k_B T} \right), \\ \delta\mathcal{F}_a^{(0;\text{th}|H)} &= \frac{2}{3\pi c^3} \left(\frac{k_B T}{\hbar} \right)^3 \sum_{b \neq a} \sum_i |\mu_i^{ab}|^2 F \left(\frac{E_a - E_b}{k_B T} \right) \end{aligned} \quad (21)$$

where the function F is given by

$$F(y) = \text{P} \int_0^\infty dx \left(\frac{1}{y+x} + \frac{1}{y-x} \right) \frac{x^3}{e^x - 1}. \quad (22)$$

$F(y)$, which is an odd function of y , is displayed in Fig.1.

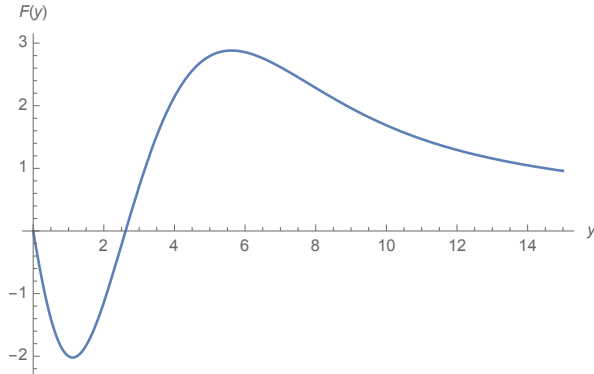


FIG. 1: Graph of the function $F(y)$ defined in Eq. (22)

In Ref. [4] it is shown that $F(y)$ has the following asymptotic behavior for small and large values of $|y|$,

$$F(y) \simeq \begin{cases} -\frac{\pi^2 y}{3} & |y| \ll 1 \\ \frac{2\pi^4}{15y} + \frac{16\pi^6}{63y^3} & |y| \gg 1 \end{cases}. \quad (23)$$

The frequency shift $\delta\nu_{aa'}^{(0;\text{th})}$ of an atom exposed to black-body radiation can be now be written as

$$\delta\nu_{aa'}^{(0;\text{th})} = \delta\nu_{aa'}^{(0;\text{th}|E)} + \delta\nu_{aa'}^{(0;\text{th}|H)}, \quad (24)$$

where

$$\delta\nu_{aa'}^{(0;\text{th}|E)} = (\delta\mathcal{F}_a^{(0;\text{th}|E)} - \delta\mathcal{F}_{a'}^{(0;\text{th}|E)})/\hbar, \quad (25)$$

$$\delta\nu_{aa'}^{(0;\text{th}|H)} = (\delta\mathcal{F}_a^{(0;\text{th}|H)} - \delta\mathcal{F}_{a'}^{(0;\text{th}|H)})/\hbar. \quad (26)$$

In Sec. V the above equations will be used to compute the shift of hyperfine transitions in free-space.

B. An atom near one or more bodies

The shifts and the radiative widths of the spectral lines of an atom in the presence of one or more bodies in thermal equilibrium with the environment can be computed using Eqs. (3) and (9), provided that the appropriate Green tensors are substituted into both equations. In systems involving a collection of bodies, the Green tensors are naturally decomposed as the sum of the free-space Green tensors, and a scattering contribution which accounts for the influence of the bodies,

$$\begin{aligned} \mathcal{E}_{ij}(\mathbf{r}, \mathbf{r}', \omega) &= \mathcal{E}_{ij}^{(0)}(\mathbf{r}, \mathbf{r}', \omega) + \mathcal{E}_{ij}^{(\text{sc})}(\mathbf{r}, \mathbf{r}', \omega), \\ \mathcal{H}_{ij}(\mathbf{r}, \mathbf{r}', \omega) &= \mathcal{H}_{ij}^{(0)}(\mathbf{r}, \mathbf{r}', \omega) + \mathcal{H}_{ij}^{(\text{sc})}(\mathbf{r}, \mathbf{r}', \omega). \end{aligned} \quad (27)$$

We note that, differently from the free-space contribution, the scattering parts of the Green tensors are non-singular in the coincidence limit $\mathbf{r} = \mathbf{r}' = \mathbf{r}_0$. Unfortunately, they are difficult to compute for general shapes and dispositions of the bodies, and their expressions are known only for a handful of special geometries. In the simple setting of two plane-parallel indefinite slabs the Green tensors can be written in terms of the Fresnel reflection coefficients of the slabs. Their explicit expressions are provided in Appendix B. The decomposition Eq. (27) implies that the energy shift $\delta\mathcal{F}_a$ can be also represented as the sum of two terms,

$$\delta\mathcal{F}_a = \delta\mathcal{F}_a^{(0;\text{bare})} + \delta\mathcal{F}_a^{(\text{sc})}, \quad (28)$$

where $\delta\mathcal{F}_a^{(0;\text{bare})}$ is identical with the free-space shift in Eq. (14) and $\delta\mathcal{F}_a^{(\text{sc})}$ has an expression analogous to Eq. (3), apart from the replacement of the Green tensors with their scattering parts. After neglecting the divergent contribution from zero-point fluctuations $\delta\mathcal{F}_a^{(0;\text{zp})}$, one arrives at the following expression for the energy shift,

$$\delta\mathcal{F}_a = \delta\mathcal{F}_a^{(0;\text{th})} + \delta\mathcal{F}_a^{(\text{sc})}. \quad (29)$$

The scattering contribution $\delta\mathcal{F}_a^{(\text{sc})}$ can be further decomposed as the sum of the dynamic Stark shift and the dynamic Zeeman shift,

$$\delta\mathcal{F}_a^{(\text{sc})} = \delta\mathcal{F}_a^{(\text{sc}|E)} + \delta\mathcal{F}_a^{(\text{sc}|H)}. \quad (30)$$

By taking advantage of the analyticity and symmetry properties of the Green tensors [7], it is possible to show that $\delta\mathcal{F}_a^{(\text{sc}|\text{E})}$ and $\delta\mathcal{F}_a^{(\text{sc}|\text{H})}$ can be recast in the following form [19],

$$\delta\mathcal{F}_a^{(\text{sc}|\text{E})} = \delta\mathcal{F}_a^{(\text{abs}|\text{E})} + \delta\mathcal{F}_a^{(\text{em}|\text{E})} + \delta\mathcal{F}_a^{(\text{non res}|\text{E})}, \quad (31)$$

$$\delta\mathcal{F}_a^{(\text{sc}|\text{H})} = \delta\mathcal{F}_a^{(\text{abs}|\text{H})} + \delta\mathcal{F}_a^{(\text{em}|\text{H})} + \delta\mathcal{F}_a^{(\text{non res}|\text{H})}, \quad (32)$$

where

$$\delta\mathcal{F}_a^{(\text{abs}|\text{E})} = \sum_{b>a} d_i^{ab} d_j^{ba} \frac{\text{Re}[\mathcal{E}_{ij}^{(\text{sc})}(\mathbf{r}_0, \mathbf{r}_0; \omega_{ba})]}{e^{\hbar\omega_{ba}/k_B T} - 1} \theta(\omega_{ba}), \quad (33)$$

$$\delta\mathcal{F}_a^{(\text{em}|\text{E})} = - \sum_{b<a} d_i^{ab} d_j^{ba} \text{Re}[\mathcal{E}_{ij}^{(\text{sc})}(\mathbf{r}_0, \mathbf{r}_0; \omega_{ab})] \frac{e^{\hbar\omega_{ab}/k_B T}}{e^{\hbar\omega_{ab}/k_B T} - 1} \theta(\omega_{ab}), \quad (34)$$

$$\delta\mathcal{F}_a^{(\text{non res}|\text{E})} = -k_B T \sum_{n=0}^{\infty} {}' \mathcal{E}_{ij}^{(\text{sc})}(\mathbf{r}_0, \mathbf{r}_0; i\xi_n) \alpha_{ij}^{(a)}(i\xi_n), \quad (35)$$

$$\delta\mathcal{F}_a^{(\text{abs}|\text{H})} = \sum_{b>a} \mu_i^{ab} \mu_j^{ba} \frac{\text{Re}[\mathcal{H}_{ij}^{(\text{sc})}(\mathbf{r}_0, \mathbf{r}_0; \omega_{ba})]}{e^{\hbar\omega_{ba}/k_B T} - 1} \theta(\omega_{ba}), \quad (36)$$

$$\delta\mathcal{F}_a^{(\text{em}|\text{H})} = - \sum_{b<a} \mu_i^{ab} \mu_j^{ba} \text{Re}[\mathcal{H}_{ij}^{(\text{sc})}(\mathbf{r}_0, \mathbf{r}_0; \omega_{ab})] \frac{e^{\hbar\omega_{ab}/k_B T}}{e^{\hbar\omega_{ab}/k_B T} - 1} \theta(\omega_{ab}), \quad (37)$$

$$\delta\mathcal{F}_a^{(\text{non res}|\text{H})} = -k_B T \sum_{n=0}^{\infty} {}' \mathcal{H}_{ij}^{(\text{sc})}(\mathbf{r}_0, \mathbf{r}_0; i\xi_n) \beta_{ij}^{(a)}(i\xi_n). \quad (38)$$

In the above Equations, $\theta(x)$ is the Heaviside function ($\theta(x) = 1$ for $x \geq 0$, and $\theta(x) = 0$ for $x < 0$), $\xi_n = 2\pi n k_B T / \hbar$, with $n = 0, 1, \dots$, are the Matsubara frequencies, and the primed sums in Eqs. (35) and (38) indicate that the $n = 0$ term is taken with a weight of one-half. The three contributions on the r.h.s. of Eqs. (31) and (32) have different physical meanings: the first terms, $\delta\mathcal{F}_a^{(\text{abs}|\text{E})}$ and $\delta\mathcal{F}_a^{(\text{abs}|\text{H})}$ respectively, correspond to virtual absorption processes by the atom, and thus they only involve virtual intermediate states b such that $E_b > E_a$. We note that $\delta\mathcal{F}_a^{(\text{abs}|\text{E})}$ and $\delta\mathcal{F}_a^{(\text{abs}|\text{H})}$ vanish for $T = 0$. The second terms, $\delta\mathcal{F}_a^{(\text{em}|\text{E})}$ and $\delta\mathcal{F}_a^{(\text{em}|\text{H})}$, correspond to virtual stimulated and spontaneous emission processes by the atom, and thus they only involve virtual intermediate states b such that $E_b < E_a$. Finally, the third contributions, $\delta\mathcal{F}_a^{(\text{non res}|\text{E})}$ and $\delta\mathcal{F}_a^{(\text{non res}|\text{H})}$, are associated with non-resonant quantum and thermal fluctuations of the atomic dipoles. The resonant contributions $\delta\mathcal{F}_a^{(\text{abs})}$ and $\delta\mathcal{F}_a^{(\text{em})}$ represent truly non-equilibrium contributions which exist only for atoms in non-thermalized states. In fact, it is possible to verify that the resonant terms $\delta\mathcal{F}_a^{(\text{abs})}$ and $\delta\mathcal{F}_a^{(\text{em})}$ both cancel out when the atom's state is fully thermalized. This can be seen from

the relation

$$\begin{aligned} \delta\mathcal{F}_{\text{CP}}^{(\text{eq})} &\equiv \frac{1}{Z} \sum_a e^{-E_a/k_B T} \delta\mathcal{F}_a^{(\text{sc})} = \frac{1}{Z} \sum_a e^{-E_a/k_B T} \delta\mathcal{F}_a^{(\text{non res})} \\ &= -k_B T \sum_{n=0}^{\infty} {}' \left[\mathcal{E}_{ij}^{(\text{sc})}(i\xi_n) \alpha_{ij}(i\xi_n) + \mathcal{H}_{ij}^{(\text{sc})}(i\xi_n) \beta_{ij}(i\xi_n) \right], \end{aligned} \quad (39)$$

where

$$Z = \sum_a \exp(-E_a/k_B T) \quad (40)$$

is the partition function (for brevity we omitted indicating the dependence of the Green tensors on the atom's position \mathbf{r}_0), and the polarizabilities of the thermalized atom are given by

$$\alpha_{ij}(i\xi_n) = \frac{1}{Z} \sum_a e^{-E_a/k_B T} \alpha_{ij}^{(a)}(i\xi_n), \quad (41)$$

$$\beta_{ij}(i\xi_n) = \frac{1}{Z} \sum_a e^{-E_a/k_B T} \beta_{ij}^{(a)}(i\xi_n) \quad (42)$$

Eq. (39) shows that when the atom is in thermal equilibrium, the (scattering contribution to the) atom's free-energy shift $\delta\mathcal{F}_{\text{CP}}^{(\text{eq})}$ coincides with the CP energy predicted by Lifshitz theory [20]. Using the expression of the

Green tensors inside a cavity provided in Appendix B, it is possible to verify that Eq. (39) indeed reproduces the formula for the interaction of a thermalized atom with a dielectric wall when the atom has a permanent magnetic moment. This result was derived in Ref. [21] by taking the dilute limit of the Lifshitz formula. The cancellation of all resonant contributions for atoms in thermal equilibrium, and the importance of a proper interpretation of the atomic polarizability have been emphasized in [13]. This becomes important when one studies non-equilibrium problems, like the CP interaction of an atom prepared in an energy eigenstate.

III. HYPERFINE STRUCTURE

In this Section, we briefly review the hyperfine structure of atomic spectra [15, 16]. We consider atoms with

one optical electron, i.e., an hydrogenic atom, or an atom with just one electron outside closed shells, like an alkali atom. The Hamiltonian \hat{H} of such an atom is given by

$$\hat{H} = \hat{H}_0 + \hat{H}_{\text{HFS}}, \quad (43)$$

where \hat{H}_0 describes the central electrostatic field of the atom and the spin-orbit interaction, while \hat{H}_{HFS} is the hyperfine Hamiltonian. It is usually possible to treat \hat{H}_{HFS} as a small perturbation to \hat{H}_0 , and then the action of \hat{H}_{HFS} can be restricted to the subspace spanned by the electronic states (nLJ) having fixed principal quantum number n , orbital quantum number L , and total electron angular momentum J . Within each (nLJ) sub-shell \hat{H}_{HFS} is of the form [15]

$$\hat{H}_{\text{HFS}} = A_J \hat{\mathbf{I}} \cdot \hat{\mathbf{J}} + \frac{B_J}{2I(2I-1)J(2J-1)} \left[3(\hat{\mathbf{I}} \cdot \hat{\mathbf{J}})^2 + \frac{3}{2} \hat{\mathbf{I}} \cdot \hat{\mathbf{J}} - I(I+1)J(J+1) \right] - \hat{\boldsymbol{\mu}} \cdot \mathbf{B}, \quad (44)$$

where \mathbf{B} is the external magnetic field, and

$$\hat{\boldsymbol{\mu}} = -g_J \mu_B \hat{\mathbf{J}} + g_I \mu_n \hat{\mathbf{I}}. \quad (45)$$

is the atom's magnetic moment. Here, $\hat{\mathbf{I}}$ and $\hat{\mathbf{J}} = \hat{\mathbf{L}} + \hat{\mathbf{S}}$ are, respectively, the nuclear spin and the total angular momentum of the electron (both expressed in units of \hbar), $\mu_B = e\hbar/2mc$ and $\mu_n = e\hbar/2Mc$ are, respectively, the Bohr and nuclear magnetons, m and M are, respectively, the electron and the proton masses, $g_J = [3J(J+1) + 3/4 - L(L+1)]/2J(J+1)$ is the electron Landé g-factor (we use for the electron gyromagnetic factor the approximate value $g = 2$), g_I is the nuclear g-factor, A_J is the magnetic hyperfine structure constant, and B_J is the electronic quadrupole interaction constant. For hydrogen the constant A_J has the value [16],

$$A_J = w_0 g_I \frac{m}{M} \frac{\alpha_e^2}{n^3} \frac{1}{J(J+1)(L+1/2)}, \quad (46)$$

where w_0 is the Bohr energy. The constant B_J is identically zero either if $I = 0$ or $1/2$, or if $J = 0, 1/2$ [15]. The latter condition implies, in particular, that B_J is zero in the ground states of the one-electron atoms that we consider.

If the external magnetic field is zero, the total angular momentum F and its projection M_F in any direction are good quantum numbers, and then the atom's states can be labelled by $|a\rangle = |nLSJ; FM_F\rangle$, where $n_a = L + n_r + 1$ ($n_r = 0, 1, 2, \dots$) is the principal quantum number, and $S = 1/2$ is the electron spin. For brevity, we shall omit from now on the quantum numbers S and I , and hence

the states of the atom in zero external magnetic field shall be denoted simply as $|a\rangle = |nLJ; FM_F\rangle$. According to Eq. (44) the energy E_F of this state is

$$E_F = E_J + \frac{1}{2} A_J K + B_J \frac{3K(K+1) - 4I(I+1)J(J+1)}{8I(2I-1)J(2J-1)}, \quad (47)$$

where E_J is the energy of the fine-structure multiplet level with electronic angular momentum J , and K is

$$K = F(F+1) - I(I+1) - J(J+1). \quad (48)$$

In our computations, we approximate E_J to order α_e^2 [26],

$$E_J = -w_0 \left[\frac{1}{n^2} + \frac{\alpha_e^2}{n^3} \left(\frac{1}{J+1/2} - \frac{3}{4n} \right) \right], \quad (49)$$

where α_e^2 is the fine structure constant. According to Eq. (47) the hyperfine interaction splits the fine-structure levels into hyperfine-structure multiplets, consisting of a number of levels equals to $2I+1$ if $J \geq I$ and $2J+1$ if $I \geq J$. For $B_J \ll A_J$ (and in particular in the ground state where $B_J = 0$) the adjacent hyperfine sub-levels are spaced by the hyperfine-structure interval ΔE

$$\Delta E = E_F - E_{F-1} = A_J F. \quad (50)$$

When the external magnetic field \mathbf{B} is different from zero, the degeneracy of the energy with respect to M_F is lifted, and the properties of the Zeeman sub-levels depend on the strength of \mathbf{B} . For weak fields such that $g_J \mu_B B \ll A_J$ (this condition is typically satisfied if B is less than 10^{-3}

T), the nuclear spin I and the electronic angular momentum J remain strongly coupled, and then the atom's eigenstates can be still labelled as $|a\rangle \equiv |nLJ; FM_F\rangle$, where M_F is the projection of the total angular momentum \mathbf{F} in the direction of \mathbf{B} . The Zeeman effect adds to Eq. (47) an energy E_{FM_F}

$$E_{FM_F} = g_F \mu_B B M_F, \quad (51)$$

where g_F is the effective g -value [15]. If the magnetic field B does not satisfy the weak-field condition $g_J \mu_B B \ll A_J$, the energy levels must be determined by resolving the secular equation for \hat{H}_{HFS} . While no general formula can be written for arbitrary values of I and J , the special case when either I or J do not exceed $1/2$ can be solved quite easily. This case is of course important, because it applies to the $^2S_{1/2}$ ground states of hydrogen and all alkali atoms. If the Zeeman sub-levels are labelled by the quantum numbers (F, M_F) of the corresponding weak-field states, the energy is given by the Breit-Rabi formula

$$E_{FM_F} = -\frac{h\nu_{\text{HFS}}}{2(2I+1)} - g_I \mu_n B M_F \pm \frac{h\nu_{\text{HFS}}}{2} \left[1 + \frac{4M_F x}{2I+1} + x^2 \right]^{1/2}, \quad (52)$$

where

$$h\nu_{\text{HFS}} = A_J(I+1/2) \quad (53)$$

is the energy separation between the ground-state sub-levels $F = I \pm 1/2$ in zero magnetic field, and the dimensionless parameter x is defined as

$$x = \frac{(g_J + g_I m/M) \mu_B B}{h\nu_{\text{HFS}}}. \quad (54)$$

In Eq. (52) the plus sign applies to states originating from the zero-field level $F = I + 1/2$, while the minus sign applies to states originating from the level $F = I - 1/2$.

Isotope	I	$\nu_{\text{HFS}}(\text{Hz})$	g_I
^1H	$1/2$	1420405751.768 ± 0.001	$5.585486(0)$
^2H	1	327384352.522 ± 0.002	$0.8574073(2)$
^3H	$1/2$	1516701470.773 ± 0.008	$5.95768(2)$

TABLE I: Values of the nuclear spin I , energy separation ν_{HFS} (in Hz) [17] and nuclear g -factor g_I for the three isotopes of hydrogen [22].

In the next Sections we shall compute the frequency shift $\delta\nu_{aa'}$ of the transitions between ground-state hyperfine sub-levels of atoms exposed to thermal radiation, both in free-space and inside a metallic cavity.

IV. SHIFT AND WIDTH OF HYPERFINE TRANSITIONS INDUCED BY BLACK-BODY RADIATION

In this Section we compute the shift $\delta\nu_{aa'}^{(0;\text{th})}$ of the transition frequencies between ground state hyperfine sub-levels of hydrogen and of its isotopes, that arise when the atom is bathed by black-body radiation in free space.

According to Eq. (24) the shift $\delta\nu_{aa'}^{(0;\text{th})}$ is the sum of two contributions, the dynamic Stark shift $\delta\nu_{aa'}^{(0;\text{th}|E)}$ and the dynamic Zeeman shift $\delta\nu_{aa'}^{(0;\text{th}|H)}$. We consider first the dynamic Zeeman shift. We see from Eqs. (21) and (26) that $\delta\nu_{aa'}^{(0;\text{th}|H)}$ involves transitions to intermediate states b that are coupled by the atom's magnetic moment $\hat{\mu}$ to the states a, a' . Since the operator $\hat{\mu}$ only acts on internal spin degrees of freedom of the electron and of the nucleus, it preserves both the principal quantum number and the orbital quantum number L , and hence

$$\begin{aligned} \mu_i^{ab} &= \langle 1, 0, 1/2; F_a M_a | \hat{\mu}_i | n_b L_b J_b; F_b M_b \rangle \\ &= \langle 1, 0, 1/2; F_a M_a | \hat{\mu}_i | 1, 0, 1/2; F_b M_b \rangle \delta_{n_b,1} \delta_{L_b,0}, \end{aligned} \quad (55)$$

where F_a and F_b are $I \pm 1/2$. Eq. (55) shows that the intermediate states b contributing to the dynamic Zeeman shift of ground state hyperfine sub-levels are the same ground state hyperfine levels. For $L_a = 0$ the electron Landé factor is $g_J = g = 2$, and then

$$\hat{\mu} = -2\mu_B \hat{\mathbf{S}} + g_I \mu_n \hat{\mathbf{I}}. \quad (56)$$

Since in a transition among ground-state hyperfine Zeeman sub-levels it holds $|E_a - E_b| \lesssim h\nu_{\text{HFS}}$, it follows that at all temperatures larger than the temperature of liquid helium the ratio $(E_b - E_a)/k_B T$ is much smaller than one (as an example, in the case of hydrogen $h\nu_{\text{HFS}}/k_B T = 0.017$ for $T = 4$ K). It is therefore possible to use in Eq. (21) the small y asymptotic expansion of F given in Eq. (23), and then we get for the dynamic Zeeman shift $\delta\mathcal{F}_a^{(0;\text{th}|H)}$ the approximate formula,

$$\begin{aligned} \delta\mathcal{F}_a^{(0;\text{th}|H)} &\simeq -\frac{8\pi}{9\hbar c^3} \left(\frac{k_B T}{\hbar} \right)^2 \mu_B^2 \\ &\times \sum_i \sum_{\substack{\text{ground} \\ b \in \text{states}}} |S_i^{ab}|^2 (E_a - E_b) \end{aligned} \quad (57)$$

By using this formula, one obtains the following estimate for the dynamic Zeeman shift $\delta\nu_{1+1/2 \rightarrow I-1/2}^{(0;\text{th}|H)}$ of the transition frequency between the states $F = I + 1/2$ and $F = I - 1/2$:

$$\delta\nu_{1+1/2 \rightarrow I-1/2}^{(0;\text{th}|H)} \simeq -\frac{2\pi}{9} \alpha_e \left(\frac{k_B T}{mc^2} \right)^2 \nu_{\text{HFS}}. \quad (58)$$

When applied to tritium, this formula gives

$$\delta\nu_{1+1/2 \rightarrow I-1/2}^{(0;\text{th}|H)} \simeq -2.0 \times \left(\frac{T}{T_{\text{room}}} \right)^2 10^{-8} \text{ Hz}. \quad (59)$$

The shifts obtained for H and D are even smaller.

Now we consider the dynamic Stark shift. For this, we need to consider the matrix elements of the electric dipole operator $\hat{\mathbf{d}}$. The selection rule $\Delta L = \pm 1$ obeyed by $\hat{\mathbf{d}}$ implies that only excited states with $L_b = 1$ have non-vanishing matrix elements with ground state levels,

$$\begin{aligned} d_i^{ab} &= \langle 1, 0, 1/2; F_a M_a | \hat{\mathbf{d}}_i | n_b, L_b, J_b; F_b M_b \rangle \\ &= \langle 1, 0, 1/2; F_a M_a | \hat{\mathbf{d}}_i | n_b, 1, J_b; F_b M_b \rangle \delta_{L_b, 1}. \end{aligned} \quad (60)$$

The explicit expression of the matrix elements d_i^{ab} can be found in Appendix A. Eq. (60) implies that for all states b such that $d_i^{ab} \neq 0$, $E_b - E_a$ is of the order of the Bohr energy $w_0 = 13.6$ eV, and then the ratio $(E_b - E_a)/k_B T$ is large ($w_0/k_B T = 526$ for $T = 300$ K). Therefore, in Eq. (21) it is possible to use the asymptotic expansion of $F(y)$ for large y . This gives

$$\begin{aligned} \delta \mathcal{F}_a^{(0; \text{th}|E)} &\simeq \frac{4\pi^3 \hbar}{45 c^3} \left(\frac{k_B T}{\hbar} \right)^4 \sum_{i,b} \frac{|d_i^{ab}|^2}{E_a - E_b} \\ &= -\frac{2\pi^3 \hbar}{45 c^3} \left(\frac{k_B T}{\hbar} \right)^4 \text{Tr} \alpha^{(a)}(0), \end{aligned} \quad (61)$$

where in the last passage we used the formula for the electric polarizability Eq. (18). By introducing the dimensionless polarizability $\tilde{\alpha}_{ij}^{(a)} = \alpha_{ij}^{(a)}/a_0^3$, where a_0 is the Bohr radius, we can recast the above formula as

$$\delta \mathcal{F}_a^{(0; \text{th}|E)} = -\frac{2\pi^3 \hbar a_0^3}{45 c^3} \left(\frac{k_B T}{\hbar} \right)^4 \text{Tr} \tilde{\alpha}^{(a)}(0). \quad (62)$$

The value of $\text{Tr} \tilde{\alpha}^{(a)}(0)$ for ground-state hyperfine levels H, D and T atoms is very close to 13.5. We thus get for the dynamic Stark shift the estimate

$$\frac{\delta \mathcal{F}_a^{(0; \text{th}|E)}}{\hbar} \simeq -\frac{\pi^2 a_0^3}{45 c^3} \left(\frac{k_B T}{\hbar} \right)^4 13.5 = -\left(\frac{T}{T_{\text{room}}} \right)^4 0.039 \text{ Hz}. \quad (63)$$

The shift of the hyperfine transition frequencies $\delta \nu_{aa'}^{(0; \text{th}|E)}$ is actually much smaller. This is so because according to Eq. (5) $\delta \nu_{aa'}^{(0; \text{th}|E)}$ actually involves the *difference* $\Delta \tilde{\alpha}_{ij}^{(aa')} = \tilde{\alpha}_{ij}^{(a)} - \tilde{\alpha}_{ij}^{(a')}$ among the polarizabilities of states a and a'

$$\delta \nu_{aa'}^{(0; \text{th}|E)} = -\frac{\pi^2 a_0^3}{45 c^3} \left(\frac{k_B T}{\hbar} \right)^4 \text{Tr} \Delta \tilde{\alpha}^{(aa')}(0). \quad (64)$$

It turns out that ground-state hyperfine sub-levels have almost identical electric polarizabilities, and therefore $\Delta \tilde{\alpha}^{(aa')}(0)$ is very small. For example, for the transition $F = I + 1/2 \rightarrow F = I - 1/2$, we find that for H, D and T the value of $\text{Tr} \Delta \tilde{\alpha}^{(aa')}(0)$ is equal to 6.9×10^{-6} , 1.6×10^{-6} and 7.3×10^{-6} , respectively. This implies that in the case of T the frequency shift has the extremely small value of:

$$\delta \nu_{1+1/2 \rightarrow I-1/2}^{(0; \text{th}|E)} = -2.1 \times \left(\frac{T}{T_{\text{room}}} \right)^4 10^{-8} \text{ Hz}. \quad (65)$$

In the case of H and D the obtained shifts are even smaller. According to Eq. (24) the total shift $\delta \nu_{aa'}^{(0; \text{th})}$ is the sum of the dynamic Zeeman shift $\delta \nu_{aa'}^{(0; \text{th}|H)}$ in Eq. (58) and the dynamic Stark shift $\delta \nu_{aa'}^{(0; \text{th}|E)}$ in Eq. (64). It is clear from Eqs. (59) and (65) that the resulting shift is too small to be measured, for practically attainable temperatures.

Finally, we consider the radiative width $\Delta \omega_{1/2}$ of the transition. Using Eq. (11) we find that $\Delta \omega_{1/2}$ is extremely small in free-space. For $T = 300$ K, $\Delta \omega_{1/2} = 2.5 \times 10^{-11}$ Hz for H, $\Delta \omega_{1/2} = 2.7 \times 10^{-12}$ Hz for D, and $\Delta \omega_{1/2} = 2.9 \times 10^{-11}$ Hz for T. The conclusion of the above findings is that the shifts $\delta \nu$ and the widths $\Delta \omega_{1/2}$ of hyperfine transitions in free space are both too small to be measurable.

V. ATOM IN A PLANAR CAVITY

In this Section we compute the energy shifts and the widths of the transitions between hyperfine ground-state Zeeman sub-levels of an atom placed inside a plane-parallel metallic cavity of width a , constituted by two identically constructed 2-layer mirrors consisting of a metallic layer of thickness w , deposited on top of a thick Si substrate. The cavity, which is in equilibrium with the environment at temperature T , is embedded in a uniform magnetic field B , whose direction is parallel to the surface of the mirrors. The z axis coincides with the direction of the B -field, while the x -axis is perpendicular to the mirrors surfaces. x is the distance of the atom from the surface of the lower mirror (see Fig. 2).

We shall study in detail the hyperfine transition $(F = 1, m_F = 0) \rightarrow (F = 0, m_F = 0)$ of H and T atoms, immersed in a weak magnetic field of about $B = 0.01$ G. The reason behind this choice is explained as follows. The computations presented below will show that the frequency shift induced by the CP interaction is rather small (of the order of a few tens of Hz). This implies that in order to have a chance for observing this little effect, it is necessary to isolate a transition which is robust against the perturbing effect of small inhomogeneities and/or uncertainties of external magnetic fields. The transition $(F = 1, m_F = 0) \rightarrow (F = 0, m_F = 0)$ satisfies precisely this requirement. In Sec. III, we indeed showed that in a weak field $B \ll A_J$ the Zeeman effect shifts the energy of the hyperfine state (F, M_F) by an amount proportional to M_F (see Eq. (51)). This implies that to first order in B , states with $M_F = 0$ are immune to the Zeeman shift, while states with $M_F \neq 0$ get shifted. This feature implies that by placing the cavity in a weak B -field, we can separate the Zeeman-sensitive transitions $(F = 1, m_F = \pm 1) \rightarrow (F = 0, m_F = 0)$ from the immune transition, without appreciably perturbing the frequency of the latter.

To get a quantitative insight of the magnitude of the external field B that achieves this goal, consider

the example of a B -field of 0.01G. Using Eq. (51) one finds that the energy of the state ($F = 1, M_F = 1$) gets shifted upwards by 14 kHz, while the energy of the state ($F = 1, M_F = -1$) gets shifted downwards by the same amount. Thus, a weak B -field of 0.01G is sufficient to separate the stable transition ($F = 1, m_F = 0$) \rightarrow ($F = 0, m_F = 0$) from both transitions involving the $M_F = \pm 1$ states. On the other hand, a B -field of 0.01G has a negligible effect on the frequency of the transition ($F = 1, m_F = 0$) \rightarrow ($F = 0, m_F = 0$). In fact, an evaluation of the exact Breit-Rabi formula Eq. (52) shows that the upper state ($F = 1, M_F = 0$) is shifted upwards by 0.14 Hz, while the lower state ($F = 0, M_F = 0$) is shifted downwards by -0.14 Hz. This implies that the B -field shifts the frequency of the ($F = 1, m_F = 0$) \rightarrow ($F = 0, m_F = 0$) transition by just 0.28 Hz, which is much smaller than the CP shift we obtain for this transition (see Figs. 3 and 5 below). After these general considerations, we turn to the computation of the shift $\delta\nu$.

As shown in Sec. II, the shift $\delta\nu_{aa'}$ of the frequency of the transition $a \rightarrow a'$ is proportional to the difference between the free energy shifts $\delta\mathcal{F}_a$ and $\delta\mathcal{F}_{a'}$ of the two states. The shifts $\delta\mathcal{F}_a$ for an atom placed in a cavity can be computed by using Eqs. (29-38), once we substitute in those equations the scattering Green functions of the cavity. The explicit formulae of these Green functions are provided in Appendix B. As it can be seen from Eqs. (B5) and (B6) the Green functions involve the reflection coefficients of the mirrors $R_\alpha^{(k)}$, which in turn involve the complex frequency-dependent permittivities $\epsilon_a(\omega)$ of the materials constituting the mirrors (see Eqs. (B7-B9)). For the permittivities we use the following models. For

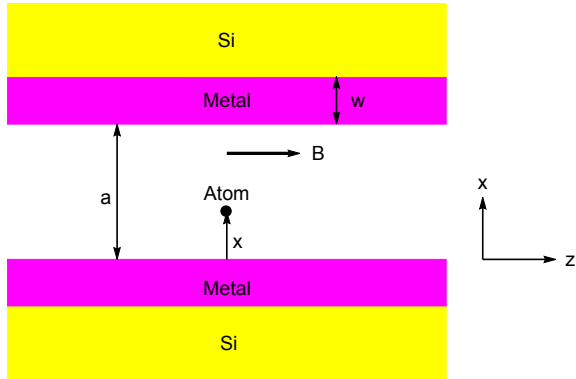


FIG. 2: Planar cavity of width a , consisting of two layered plane-parallel metallic mirrors. The atom is at distance x from the lower mirror. The uniform magnetic field B is directed along the z direction.

the metals, we used the simple Drude model

$$\epsilon_{\text{Dr}}(\omega) = 1 - \frac{\Omega_p^2}{\omega(\omega + i\gamma)}, \quad (66)$$

where Ω_p and γ are, respectively, the plasma and the re-

laxation frequencies. This simple model is adequate for our problem, because it turns out that up-to negligible terms, the shifts $\delta\mathcal{F}_a$ are determined by the resonant contribution to the dynamic Zeeman effect, which according to Eq. (38) involves the values of the Green tensors at the frequencies of the hyperfine transitions. The latter frequencies belong to the GHz region, where the Drude model provides an accurate description of the electromagnetic response of metals.

We recall that the plasma frequency Ω_p is independent of temperature, while the relaxation frequency is temperature dependent [23]. It is well known [23] that in the range of temperatures $T_D/4 < T < T_{\text{room}} = 300\text{K}$, where T_D is the Debye temperature, the relaxation frequency depends linearly on the temperature,

$$\gamma = \gamma_{\text{room}}[1 + (T - T_{\text{room}})\alpha]. \quad (67)$$

At lower temperatures, γ reaches a saturation value $\gamma_s = \gamma_{\text{room}}/\text{RRR}$ where the RRR ratio is determined by the amount of impurities, which depends on sample preparation. In ultra-clean samples, and for temperatures extending from $T_D/4$ down to liquid helium temperature, $\gamma(T)$ decreases like T^5 , in accordance with the Bloch-Grüneisen law [24]. At even lower temperatures $\gamma(T) \sim T^2$ for metals with perfect crystal lattices [23]. In Table II we list the values of the Drude parameters, Debye temperature and the thermal coefficient α for some metals. In the numerical computations for $T = 70\text{ K}$ presented below, we set $\gamma = \gamma_{\text{room}}/\text{RRR}$ for all considered metals.

Metal	$\Omega_p(\text{eV}/\hbar)$	$\gamma_{\text{room}}(\text{eV}/\hbar)$	$\alpha \times 10^3(\text{K}^{-1})$	$T_D(\text{K})$
Au	9	0.035	3.4	165
Al	11.5	0.050	4.3	428
Ag	9.014	0.018	4.0	225
Pt	4.89	0.07	3.9	240

TABLE II: Values of the Drude parameters [25], Debye temperatures T_D [23] and thermal coefficients α for some metals.

For the permittivity of the Si substrate we used the formula [23]

$$\epsilon_{\text{Si}}(\omega) = \epsilon_\infty + \frac{\omega_{\text{UV}}^2}{\omega_{\text{UV}}^2 - \omega^2 - i\omega\gamma_{\text{Si}}}(\epsilon_0 - \epsilon_\infty), \quad (68)$$

with $\epsilon_\infty = 1.035$, $\epsilon_0 = 11.67$, $\omega_{\text{UV}} = 6.6 \times 10^{15} \text{ rad/s}$, and $\gamma_{\text{Si}} = 1.52 \times 10^{12} \text{ rad/s}$.

We are now ready to compute the shift $\delta\nu_{aa'}$ of the hyperfine transition of an atom placed inside the cavity. According to Eq. (29) the shift $\delta\nu_{ab}$ is the sum of the free-space shift $\delta\nu_{aa'}^{(0;\text{th})}$ and a scattering contribution $\delta\nu_{aa'}^{(\text{sc})}$,

$$\delta\nu_{aa'} = \delta\nu_{aa'}^{(0;\text{th})} + \delta\nu_{aa'}^{(\text{sc})}. \quad (69)$$

The free-space shift $\delta\nu_{aa'}^{(0;\text{th})}$ was computed in the previous Section and was found to be negligible. In view of

Eqs. (33-38) the scattering contribution $\delta\nu_{aa'}^{(\text{sc})}$ to the shift is the sum of six terms which are written as

$$\begin{aligned} \delta\nu_{aa'}^{(\text{sc})} = & \delta\nu_{aa'}^{(\text{abs}|E)} + \delta\nu_{aa'}^{(\text{em}|E)} + \delta\nu_{aa'}^{(\text{non res}|E)} \\ & + \delta\nu_{aa'}^{(\text{abs}|H)} + \delta\nu_{aa'}^{(\text{em}|H)} + \delta\nu_{aa'}^{(\text{non res}|H)}. \end{aligned} \quad (70)$$

Since we are interested in the shifts of ground-state hyperfine transitions, both states a and a' are ground-state hyperfine sub-levels. This implies at once that

$$\delta\nu_{aa'}^{(\text{em}|E)} = 0. \quad (71)$$

The above identity is a consequence of the fact that for any ground-state level a the shift $\delta\mathcal{F}_a^{(\text{em}|E)}$ in Eq. (34) vanishes identically. This is so because the intermediate states b that contribute to $\delta\mathcal{F}_a^{(\text{em}|E)}$ must have a lower energy than a , and therefore they are ground-state hyperfine levels. However the matrix elements of the electric-dipole operators between two ground-state levels are zero, and therefore $\delta\mathcal{F}_a^{(\text{em}|E)}$ vanishes. Next, we consider the contribution $\delta\nu_{aa'}^{(\text{abs}|E)}$. This term is negligible, since according to Eq. (33) it only involves intermediate states b that are coupled to the ground-state hyperfine sub-levels a and a' by the electric-dipole operator. Because of the selection rule $\Delta L = \pm 1$, these intermediate states are excited states with $L = 1$, and then for the temperatures that we consider, the Bose factor $[\exp(\hbar\omega_{ab}/k_B T) - 1]^{-1} \simeq [\exp(w_0/k_B T) - 1]^{-1} \ll 1$ leads to a strong suppression of $\delta\nu_{aa'}^{(\text{abs}|E)}$. Next, we consider $\delta\nu_{aa'}^{(\text{non res}|E)}$. According to Eq. (35), this contribution can be recast in the form

$$\delta\nu_{aa'}^{(\text{non res}|E)} = -k_B T a_0^3 \sum_{n=0}^{\infty} \mathcal{E}_{ij}^{(\text{sc})}(\mathbf{r}_0, \mathbf{r}_0; i\xi_n) \Delta\tilde{\alpha}_{ij}^{(aa')}(i\xi_n). \quad (72)$$

We pointed out earlier that the electric polarizabilities $\tilde{\alpha}_{ij}^{(a)}$ of ground-state hyperfine sub-levels are almost identical to each other. Because of this feature the shift $\delta\nu_{aa'}^{(\text{non res}|E)}$ is very small. As an example, consider the transition $(F=1, m_F=0) \rightarrow (F=0, m_F=0)$ of an H atom placed in a Au cavity at room temperature, having a width a of one micron, in zero magnetic field. If the atom is placed at the center of the cavity (i.e. for $x = a/2$), we find $\delta\nu_{1,0;0,0}^{(\text{non res}|E)} = -1.3 \times 10^{-4}$ Hz. If the atom is moved at a distance $x = 200$ nm from the lower mirror, we find $\delta\nu_{1,0;0,0}^{(\text{non res}|E)} = -2.4 \times 10^{-3}$ Hz. Shifts of a comparably small magnitude are obtained also for the other transitions, as well as for D and T. The above considerations show that the dynamic Stark shift of the ground-state hyperfine transition frequencies is negligibly small.

We consider now the dynamic Zeeman shift. It turns out that the non-resonant contribution $\delta\nu_{aa'}^{(\text{non res}|H)}$ is always very small, compared to the resonant contribution $\delta\nu_{aa'}^{(\text{res}|H)} = \delta\nu_{aa'}^{(\text{abs}|H)} + \delta\nu_{aa'}^{(\text{em}|H)}$. Consider again the transition $(F=1, m_F=0) \rightarrow (F=0, m_F=0)$ of an H atom

placed in a Au cavity, under the same conditions considered above. At room temperature, the non-resonant shift for $x = a/2$ is $\delta\nu_{aa'}^{(\text{non res}|H)} = -3.14 \times 10^{-6}$ Hz, to be contrasted with $\delta\nu_{aa'}^{(\text{res}|H)} = 7.44$ Hz. Similarly, for $x = 200$ nm we find $\delta\nu_{aa'}^{(\text{non res}|H)} = -2.15 \times 10^{-5}$ Hz, while $\delta\nu_{aa'}^{(\text{res}|H)} = 8.31$ Hz. For $T = 70$ K, and for $x = a/2$ we find $\delta\nu_{aa'}^{(\text{non res}|H)} = -1.6 \times 10^{-5}$ Hz, to be contrasted with $\delta\nu_{aa'}^{(\text{res}|H)} = 10.12$ Hz, while for $x = 200$ nm we find $\delta\nu_{aa'}^{(\text{non res}|H)} = -9.8 \times 10^{-5}$ Hz, and $\delta\nu_{aa'}^{(\text{res}|H)} = 12.9$ Hz. From this we conclude that, up to negligible corrections, the shift $\delta\nu_{aa'}$ of the hyperfine ground-state transitions is entirely due to the resonant contributions to the dynamic Zeeman effect, i.e.,

$$\delta\nu_{aa'} \simeq \delta\nu_{aa'}^{(\text{res}|H)} \equiv \delta\nu_{aa'}^{(\text{abs}|H)} + \delta\nu_{aa'}^{(\text{em}|H)}. \quad (73)$$

An important feature of the above result is its *robustness*. Since the dynamic Zeeman shifts of the free-energies $\delta\mathcal{F}_a^{(\text{abs}|H)}$ and $\delta\mathcal{F}_a^{(\text{em}|H)}$ depend only on the hyperfine transition frequencies ω_{ab} (see Eqs. (36)) and (37)), it is clear that the frequency shift $\delta\nu_{aa'}$ is independent of the value of the constant E_J in Eq. (47), whose effect is to just shift the energies of the hyperfine levels by an irrelevant overall constant, which does not change the hyperfine transition frequencies ω_{ab} . This implies that the inclusion in E_J of higher order corrections in α_e , like for example for the Lamb shift, is irrelevant as far as they are independent of the total angular momentum F . The transition frequencies ω_{ab} are determined solely by the experimentally known frequency ν_{HFS} and by the magnetic field B , in accordance with the Breit-Rabi formula in Eq. (52).

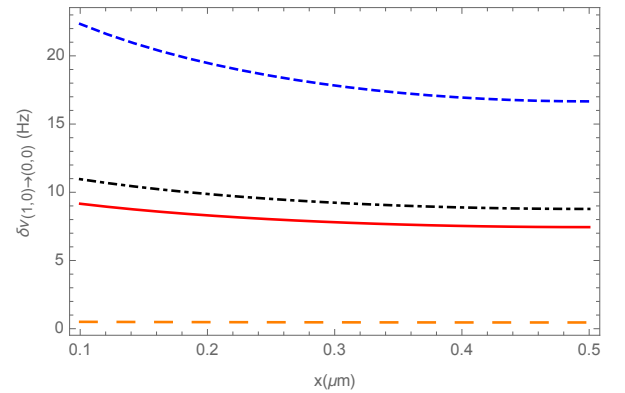


FIG. 3: Shift $\delta\nu$ (in Hz) of the H hyperfine transition $(F=1, m_F=0) \rightarrow (F=0, m_F=0)$ (in Hz), versus the minimum atom-mirror separation x (in micron). The atom is placed inside a metallic cavity of width $a = 1$ micron at room temperature, in a magnetic field $B=0.01$ G. The thickness of the metallic layer is 5 micron. The four curves, from top to bottom, are for a cavity made of Ag, Al, Au and Pt, respectively.

The results of our numerical computations are displayed in Figs. 3 to 9. In Fig. 3 and in Fig. 5 we show

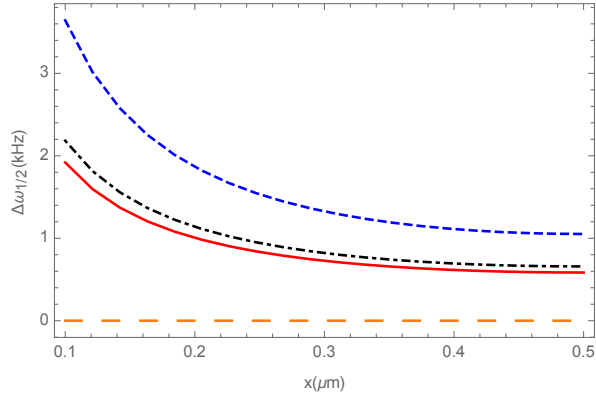


FIG. 4: Half-width $\Delta\omega_{1/2}$ (in kHz) of the H hyperfine transition ($F = 1, m_F = 0 \rightarrow F = 0, m_F = 0$) (in Hz), versus the minimum atom-mirror separation x (in micron). The atom is placed inside a metallic cavity of width $a = 1$ micron at room temperature, in a magnetic field $B=0.01G$. The metallic layers have a thickness $w=5$ micron. The four curves, from top to bottom, are for a cavity made of Ag, Al, Au and Pt, respectively.

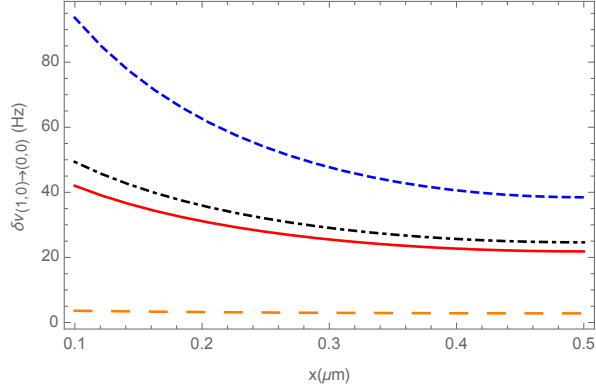


FIG. 5: Shift $\delta\nu$ (in Hz) of the H hyperfine transition ($F = 1, m_F = 0 \rightarrow F = 0, m_F = 0$) (in Hz), versus the minimum atom-mirror separation x (in micron). The atom is placed inside a metallic cavity of width $a = 1$ micron at a temperature $T = 70$ K (RRR=10), in a magnetic field $B=0.01G$. The metallic layers have a thickness $w=5$ micron. The four curves, from top to bottom, are for a cavity made of Ag, Al, Au and Pt, respectively.

the shift $\delta\nu$ (in Hz) versus separation x (in micron) of the hyperfine transition ($F = 1, m_F = 0 \rightarrow F = 0, m_F = 0$) of an H atom placed in a metallic cavity having a width a of one micron, in a magnetic field $B=0.01G$. The temperature of the cavity is $T = 300K$ in Fig. 3, and $T = 70K$ (assuming an RRR ratio of 10) in Fig. 5. The four displayed curves, from top to bottom, are for a cavity made of Ag, Al, Au and Pt, respectively. The metallic layers have a thickness $w=5$ micron. In Fig. 4 and in Fig. 6 we display the respective half-widths $\Delta\omega_{1/2}$ (in kHz). Comparison of Fig. 5 with Fig. 3 shows that the magnitude of the shift $\delta\nu$ increases as the temperature of the cavity is decreased. This behavior is explained by the fact that

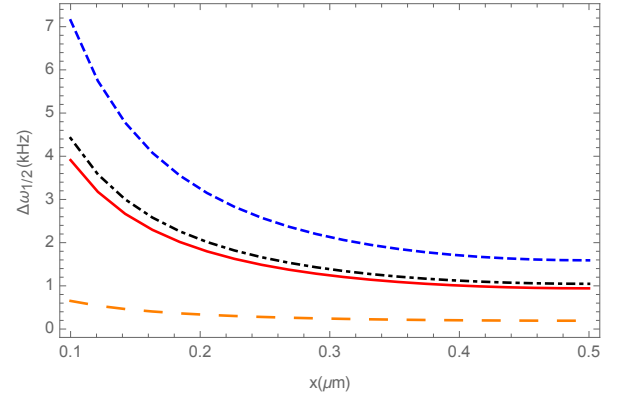


FIG. 6: Half-width $\Delta\omega_{1/2}$ (in kHz) of the H hyperfine transition ($F = 1, m_F = 0 \rightarrow F = 0, m_F = 0$) (in Hz), versus the minimum atom-mirror separation x (in micron). The atom is placed inside a metallic cavity of width $a = 1$ micron at a temperature $T = 70$ K (RRR=10), in a magnetic field $B=0.01G$. The metallic layers have a thickness $w=5$ micron. The four curves, from top to bottom, are for a cavity made of Ag, Al, Au and Pt, respectively.

the conductivity of the mirrors becomes larger at lower temperatures. This is further demonstrated by Fig. (7) which displays the shift for an H atom at a distance of 100nm from one of the mirrors, as a function of the RRR ratio of the mirrors, for $T = 70$ K. Fig. 8 displays the corresponding behavior for the rate, which also increases with RRR. The results obtained for T are not shown here as they are similar to those for H.

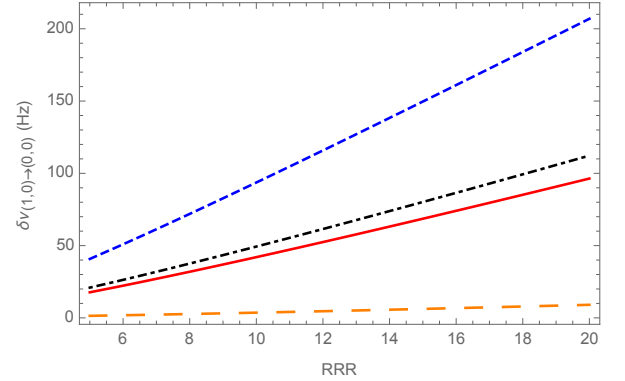


FIG. 7: Shift $\delta\nu$ (in Hz) of the H hyperfine transition ($F = 1, m_F = 0 \rightarrow F = 0, m_F = 0$) (in Hz), versus the RRR ratio of the mirrors. The atom is placed at a distance $x=100$ nm from one of the mirrors of a metallic cavity of width $a = 1$ micron at a temperature $T = 70$ K, in a magnetic field $B=0.01G$. The metallic layers have a thickness $w=5$ micron. The four curves, from top to bottom, are for a cavity made of Ag, Al, Au and Pt, respectively.

In Fig. 9 we finally plot the shift $\delta\nu$ (in Hz) of the hyperfine transition ($F = 1, m_F = 0 \rightarrow F = 0, m_F = 0$) an H atom placed at a distance $x = 200$ nm from one of the mirrors of a metallic cavity of width $a = 1$ micron at

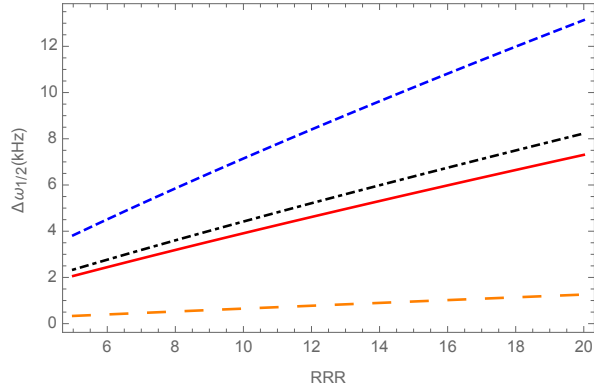


FIG. 8: Half-width $\Delta\omega_{1/2}$ (in kHz) of the H hyperfine transition ($F = 1, m_F = 0 \rightarrow F = 0, m_F = 0$) (in Hz), versus the RRR ratio of the mirrors. The atom is placed at a distance $x=100$ nm from one of the mirrors of a metallic cavity of width $a = 1$ micron at temperature $T = 70$ K, in a magnetic field $B=0.01$ G. The metallic layers have a thickness $w=5$ micron. The four curves, from top to bottom, are for a cavity made of Ag, Al, Au and Pt, respectively.

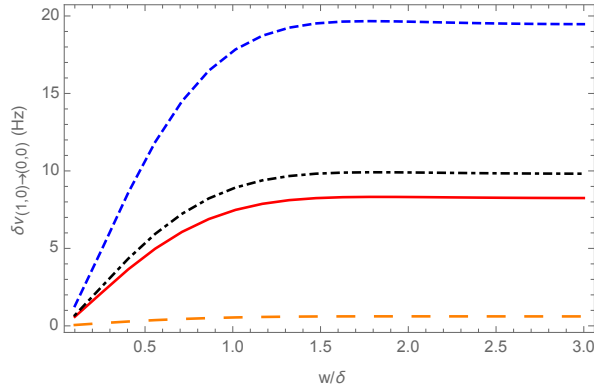


FIG. 9: Shift $\delta\nu$ (in Hz) of the hyperfine transition ($F = 1, m_F = 0 \rightarrow F = 0, m_F = 0$) of an H atom placed at a distance $x = 200$ nm from one of the mirrors of a metallic cavity of width $a = 1$ micron at room temperature, versus the thickness w of the metallic layer (in units of the skin depth δ corresponding to the frequency ν_{HFS}). The external magnetic field is $B=0.01$ G. The four curves, from top to bottom, are for a cavity made of Ag, Al, Au and Pt, respectively.

room temperature, versus the thickness w of the metallic layer, divided by the skin depth $\delta = c/2\pi\sqrt{\nu_{\text{HFS}}\sigma}$ corresponding to the frequency ν_{HFS} . The four curves, from top to bottom, are for a cavity made of Ag, Al, Au and Pt, respectively. The respective values of the skin depths are $\delta = 1.7 \mu\text{m}$, $2.2 \mu\text{m}$, $2.4 \mu\text{m}$ and $6.2 \mu\text{m}$. The plot shows that for a thickness w of the metallic layer approximately equal to twice the skin depth the obtained shift $\delta\nu$ is indistinguishable from that of an infinitely thick mirror.

VI. CONCLUSIONS

The Casimir-Polder interaction of an atom prepared in a well-defined energy state may deviate strongly from the Casimir-Polder energy predicted by Lifshitz theory for a fully thermalized atom, as a result of resonant virtual-photon absorption and emission processes, that are absent when the atom is in a thermal equilibrium state. This non-equilibrium interaction can be measured by spectroscopic means, by observing frequency shifts suffered by atoms inside a cavity. In this paper we computed the frequency shift of ground-state hyperfine transitions of an H atom placed in a metallic cavity at finite temperature. We found that the resonant Casimir-Polder interaction of the atom's magnetic moment with the fluctuating magnetic field existing in the cavity causes a significant shift of hyperfine transitions, and it also leads to a very large increase of their widths, as compared to an atom in free-space exposed to black-body radiation at the same temperature as the cavity. By considering cavities made of different metals and hold at different temperatures, we established that larger frequency shifts are obtained in cavities made of metals having a large conductivity, most notably Ag and Al at low temperatures. The predicted shifts for H atoms placed at a distance of a hundred nanometers from the walls of a Ag cavity at a temperature of 70K can be as large as 90 Hz, while their widths are of the order of a few kHz. The obtained shift could be measurable with presently available techniques of magnetic resonance. The main experimental challenge for observing the effect is to find means of placing the atom at a well-defined position in a metallic cavity, for a sufficiently long time as is necessary to measure a frequency shift of a few tens of Hz. The experimental investigation of this problem might shed light on open questions about the temperature dependence of dispersion forces between lossy media [12].

Appendix A: Matrix elements of the dipole operators

In this Appendix, we compute the matrix elements of the operators $\hat{\mu}$ and $\hat{\mathbf{d}}$, that are needed for the computation of the shift of ground state hyperfine levels of hydrogen.

1. Magnetic-dipole matrix elements

We start from the magnetic-dipole moment. According to Eq. (55), the operators $\hat{\mu}_i$ only connect the ground state hyperfine sub-levels among themselves. For brevity, we shall suppress the quantum numbers $n = 1$, $L = 0$ and $J = 1/2$ which pertain to the ground state, and thus we shall denote the state $|1, 0, 1/2; F_a M_a\rangle$ as $|F_a M_a\rangle$. For

$L_a = 0$, one has the identity

$$\hat{\mu}_i = g_I \mu_n \hat{F}_i - (g_J \mu_B + g_I \mu_n) \hat{S}_i. \quad (A1)$$

Using this identity, we obtain

$$\begin{aligned} \langle F_a M_a | \hat{\mu}_i | F_b M_b \rangle &= g_I \mu_n \langle F_a M_a | \hat{F}_i | F_a M_b \rangle \delta_{F_a F_b} \\ &\quad - (g_J \mu_B + g_I \mu_n) \langle F_a M_a | \hat{S}_i | F_b M_b \rangle \end{aligned} \quad (A2)$$

In the ground state, F_a and F_b can take the values $I \pm 1/2$, and then two cases are possible: either $F_a = F_b$, or $F_a = I + 1/2$ and $F_b = I - 1/2$ (the case $F_a = I - 1/2$ and $F_b = I + 1/2$ is related by hermiticity to the previous one). If $F_a = F_b$, the Wigner-Eckart theorem implies the identity

$$\langle F_a M_a | \hat{S}_i | F_a M_b \rangle = \tau_{F_a} \langle F_a M_a | \hat{F}_i | F_a M_b \rangle \quad (A3)$$

The number τ_{F_a} can be computed as follows. Upon multiplying both members by $\langle F_a M_c | \hat{F}_i | F_a M_a \rangle$ and then summing over i and a , one gets

$$\langle F_a M_c | \hat{\mathbf{F}} \cdot \hat{\mathbf{S}} | F_a M_a \rangle = \tau_{F_a} \langle F_a M_a | \hat{\mathbf{F}}^2 | F_a M_b \rangle \quad (A4)$$

Using the following identity, which holds for $L_a = 0$,

$$\hat{\mathbf{F}} \cdot \hat{\mathbf{S}} = \frac{1}{2} \left[\hat{\mathbf{F}}^2 + \hat{\mathbf{S}}^2 - (\hat{\mathbf{F}} - \hat{\mathbf{S}})^2 \right] = \frac{1}{2} \left[\hat{\mathbf{F}}^2 + \hat{\mathbf{S}}^2 - \hat{\mathbf{I}}^2 \right], \quad (A5)$$

it follows that

$$\tau_{F_a} = \frac{F(F+1) + 3/4 - I(I+1)}{2F(F+1)}. \quad (A6)$$

By combining Eq. (A6) with Eqs. (A3) and (A2), one finds

$$\begin{aligned} \langle F_a M_a | \hat{\mu}_i | F_a M_b \rangle &= \left[g_I \mu_n \frac{F(F+1) - 3/4 + I(I+1)}{2F(F+1)} \right. \\ &\quad \left. - g_J \mu_B \frac{F(F+1) + 3/4 - I(I+1)}{2F(F+1)} \right] \langle F_a M_a | \hat{F}_i | F_a M_b \rangle. \end{aligned} \quad (A7)$$

The matrix elements of \hat{F}_i have the well-known expressions [26]

$$\begin{aligned} \langle F_a M_a | \hat{F}_x | F_a M_b \rangle &= \frac{1}{2} \left(\sqrt{(F_a - M_b)(F_a + M_b + 1)} \delta_{M_a, M_b+1} \right. \\ &\quad \left. + \sqrt{(F_a + M_b)(F_a - M_b + 1)} \delta_{M_a, M_b-1} \right) \end{aligned} \quad (A8)$$

$$\begin{aligned} \langle F_a M_a | \hat{F}_y | F_a M_b \rangle &= \frac{1}{2i} \left(\sqrt{(F_a - M_b)(F_a + M_b + 1)} \delta_{M_a, M_b+1} \right. \\ &\quad \left. - \sqrt{(F_a + M_b)(F_a - M_b + 1)} \delta_{M_a, M_b-1} \right) \end{aligned} \quad (A9)$$

and

$$\langle F_a M_a | \hat{F}_z | F_a M_b \rangle = M_a \delta_{M_a, M_b}. \quad (A10)$$

Next, we consider the case $F_a = I + 1/2$ and $F_b = I - 1/2$. Then Eq. (A2) implies

$$\begin{aligned} \langle I+1/2, M_a | \hat{\mu}_i | I-1/2, M_b \rangle &= \langle I-1/2, M_b | \hat{\mu}_i | I+1/2, M_a \rangle^* \\ &= -(g_J \mu_B + g_I \mu_n) \langle I+1/2, M_a | \hat{S}_i | I-1/2, M_b \rangle \end{aligned}$$

The matrix elements of the spin operators \hat{S}_i can be easily computed by expressing the states $|F_b M_b\rangle$ as linear combinations of the states $|M_I M_S\rangle'$ which are eigenstates of \hat{I}_z and \hat{S}_z [26]

$$\begin{aligned} |I+1/2, M_b\rangle &= \left(\frac{I+M_b+1/2}{2I+1} \right)^{1/2} |M_b-1/2, 1/2\rangle' \\ &\quad + \left(\frac{I-M_b+1/2}{2I+1} \right)^{1/2} |M_b+1/2, -1/2\rangle', \\ |I-1/2, M_b\rangle &= - \left(\frac{I-M_b+1/2}{2I+1} \right)^{1/2} |M_b-1/2, 1/2\rangle' \\ &\quad + \left(\frac{I+M_b+1/2}{2I+1} \right)^{1/2} |M_b+1/2, -1/2\rangle'. \end{aligned}$$

By a simple algebra, one finds

$$\begin{aligned} \langle I+1/2, M_a | \hat{S}_x | I-1/2, M_b \rangle &= \frac{\sqrt{(I+M_b+3/2)(I+M_b+1/2)}}{2(2I+1)} \delta_{M_a, M_b+1} \\ &\quad - \frac{\sqrt{(I-M_b+3/2)(I-M_b+1/2)}}{2(2I+1)} \delta_{M_a, M_b-1} \end{aligned}$$

$$\begin{aligned} \langle I+1/2, M_a | \hat{S}_y | I-1/2, M_b \rangle &= \frac{1}{i} \left\{ \frac{\sqrt{(I+M_b+3/2)(I+M_b+1/2)}}{2(2I+1)} \delta_{M_a, M_b+1} \right. \\ &\quad \left. + \frac{\sqrt{(I-M_b+3/2)(I-M_b+1/2)}}{2(2I+1)} \delta_{M_a, M_b-1} \right\} \end{aligned}$$

$$\langle I+1/2, M_a | \hat{S}_z | I-1/2, M_b \rangle = - \frac{\sqrt{(I+1/2)^2 - M_b^2}}{(2I+1)} \delta_{M_a, M_b}$$

2. Electric-dipole matrix elements

In this Section we work out the matrix elements of the electric-dipole moment operators \hat{d}_i that are needed for the computation of the Stark effect of ground-state hyperfine levels. The operators \hat{d}_x , \hat{d}_y and \hat{d}_z obey the selection rule $\Delta L = \pm 1$, and thus they connect the ground-state hyperfine sub-levels, which have $L = 0$, with excited states having $L = 1$

$$d_i^{ab} = \langle 1, 0, 1/2; F_a M_a | \hat{d}_i | n_b, 1, J_b; F_b M_b \rangle. \quad (A11)$$

To compute these matrix elements, it is convenient to first factorize d_i^{ab} into radial and an angular parts,

$$d_i^{ab} = -e a_0 R_{n_b 1}^{10} \left\langle 1, 0, 1/2; F_a M_a \left| \frac{\hat{x}_i}{r} \right| n_b, 1, J_b; F_b M_b \right\rangle \quad (A12)$$

where a_0 is the Bohr radius, r is the radial coordinate, and $R_{n_b L_b}^{n_a L_a}$ denote the radial integrals

$$R_{n_b L_b}^{n_a L_a} = \frac{1}{a_0} \int_0^\infty dr r^3 R_{n_b L_b}^*(r) R_{n_a L_a}(r). \quad (\text{A13})$$

Here $R_{n_a L_a}(r)$ and $R_{n_b L_b}(r)$ are the radial parts of the atomic wave function. For hydrogen the integrals $R_{n_b L_b}^{n_a L_a}$ can be expressed in terms of confluent hypergeometric functions [27]. For discrete energy states they have the simple expression

$$|R_{n1}^{10}| = 16 \sqrt{\frac{n^7 (n-1)^{2n-5}}{(n+1)^{2n+5}}}. \quad (\text{A14})$$

The radial integrals are more involved for continuum states. States of energy $E > 0$ can be labelled by the positive real number $\tilde{k} = ka_0$, where $k = \sqrt{2mE}/\hbar$. With this parametrization, the radial wave functions $R_{\tilde{k}l}(r)$ of continuum states are normalized [29] such that

$$\langle R_{\tilde{k}'l} | R_{\tilde{k}l} \rangle = \int_0^\infty dr r^2 R_{\tilde{k}'l}^*(r) R_{\tilde{k}l}(r) = \delta(\tilde{k}' - \tilde{k}). \quad (\text{A15})$$

Then one finds

$$\begin{aligned} |R_{\tilde{k}1}^{10}| &= \left| \frac{1}{a_0} \int_0^\infty dr r^3 R_{\tilde{k}1}^*(r) R_{10}(r) \right| \\ &= \frac{4}{3} \frac{1}{\tilde{k}^4} \sqrt{\frac{\tilde{k} + 1/\tilde{k}}{1 - \exp(-2\pi/\tilde{k})}} |I(\tilde{k})|, \end{aligned} \quad (\text{A16})$$

where $I(\tilde{k})$ is the integral

$$I(\tilde{k}) = \int_0^\infty dx x^4 e^{-(i+1/\tilde{k})x} \Phi(2 + i/\tilde{k}; 4; 2ix). \quad (\text{A17})$$

Here, $\Phi(a; c; x)$ is the *confluent hypergeometric function*. The integral $I(\tilde{k})$ can be expressed in terms of the hypergeometric function ${}_2F_1(a, b; c; z)$. The lengthy formula is omitted for brevity.

Now, we consider the matrix elements of the angular operators \hat{d}_i/r . They can be expressed as

$$\begin{aligned} \frac{\hat{x}}{r} &= \frac{\hat{C}_{-1}^1 - \hat{C}_1^1}{\sqrt{2}}, \\ \frac{\hat{y}}{r} &= i \frac{\hat{C}_{-1}^1 + \hat{C}_1^1}{\sqrt{2}}, \\ \frac{\hat{z}}{r} &= \hat{C}_0^1, \end{aligned} \quad (\text{A18})$$

where \hat{C}_q^l denote the multiplication operators by the normalized spherical harmonics

$$C_q^l := \sqrt{\frac{4\pi}{2l+1}} Y_q^l \quad (\text{A19})$$

To compute the matrix elements of the operators \hat{C}_q^l , it is useful to introduce two more sets of states. Let

$\hat{\mathbf{G}} = \hat{\mathbf{S}} + \hat{\mathbf{I}}$ be the sum of the electron and nuclear spin operators. We let $|n, L, G; \text{FM}\rangle'$ the states which are eigenstates of $\hat{\mathbf{G}}^2$. Moreover, we consider the states $|n; L, M_L; \text{GM}_G\rangle''$ that are eigenstates of \hat{L}_z , $\hat{\mathbf{G}}^2$ and \hat{G}_z . Since for $L = 0$ it holds $G = F$ and $M_G = M_F$ it follows that

$$\begin{aligned} \hat{C}_q^1 |1, 0, 1/2; F_a M_a\rangle &= \hat{C}_q^1 |1; 0, 0; F_a M_a\rangle'' \\ &= \frac{1}{\sqrt{3}} |1; 1, q; F_a M_a\rangle'' \\ &= \frac{1}{\sqrt{3}} \sum_{F_c, M_c} |n, 1, F_a; F_c M_c\rangle' \langle F_c M_c | 1, q; F_a M_a \rangle, \end{aligned} \quad (\text{A20})$$

where $\langle F_c M_c | 1, q; F_a M_a \rangle$ is a Clebsch-Gordan coefficient. At this point, using the “6j” symbols [26] we express the state $|n_b, 1, J_b; F_b M_b\rangle$ as a combination of the states $|n_b, 1, G; F_b M_b\rangle'$

$$\begin{aligned} |n_b, 1, J_b; F_b M_b\rangle &= \sum_G |n_b, 1, G; F_b M_b\rangle' \sqrt{(2J_b+1)(2G+1)} \\ &\times (-1)^{3/2+I+F_b} \begin{Bmatrix} 1 & 1/2 & J_b \\ I & F_b & G \end{Bmatrix}. \end{aligned} \quad (\text{A21})$$

By combining Eq. (A20) and (A21) we obtain

$$\begin{aligned} \langle 1, 0, 1/2; F_a M_a | \hat{C}_q^1 | n_b, 1, J_b; F_b M_b \rangle &= \frac{1}{\sqrt{3}} \sqrt{(2J_b+1)(2F_a+1)} (-1)^{3/2+I+F_b} \\ &\times \begin{Bmatrix} 1 & 1/2 & J_b \\ I & F_b & F_a \end{Bmatrix} \langle 1, q; F_a M_a | F_b M_b \rangle. \end{aligned} \quad (\text{A22})$$

Appendix B: Green function of a planar cavity

In this Appendix we provide the explicit formulae for the Green functions of a cavity, that are needed for the computations described in the present work.

At points \mathbf{r} and \mathbf{r}' in the gap between two parallel dielectric slabs at distance a in vacuum, the electric Green function $\mathcal{E}_{ij}(\mathbf{r}, \mathbf{r}', \omega)$ can be decomposed as

$$\mathcal{E}_{ij}^{(\text{cav})}(\mathbf{r}, \mathbf{r}', \omega) = \mathcal{E}_{ij}^{(0)}(\mathbf{r}, \mathbf{r}', \omega) + \mathcal{E}_{ij}^{(\text{sc})}(\mathbf{r}, \mathbf{r}', \omega), \quad (\text{B1})$$

where $\mathcal{E}_{ij}^{(0)}(\mathbf{r}, \mathbf{r}', \omega)$ is the free-space Green function, and $\mathcal{E}_{ij}^{(\text{sc})}(\mathbf{r}, \mathbf{r}', \omega)$ is a scattering contribution. The magnetic Green function has an analogous decomposition

$$\mathcal{H}_{ij}^{(\text{cav})}(\mathbf{r}, \mathbf{r}', \omega) = \mathcal{H}_{ij}^{(0)}(\mathbf{r}, \mathbf{r}', \omega) + \mathcal{H}_{ij}^{(\text{sc})}(\mathbf{r}, \mathbf{r}', \omega). \quad (\text{B2})$$

The free-space Green function has the expression

$$\mathcal{E}^{(0)}(\mathbf{r}, \mathbf{r}', \omega) = \mathcal{H}^{(0)}(\mathbf{r}, \mathbf{r}', \omega) = \left[(3\hat{\mathbf{R}} \otimes \hat{\mathbf{R}} - \mathbf{1}) \left(\frac{1}{R^3} - \frac{i\omega}{cR^2} \right) \right]$$

$$+ (\mathbf{1} - \hat{\mathbf{R}} \otimes \hat{\mathbf{R}}) \frac{\omega^2}{c^2 R} - \frac{4\pi}{3} \delta(\mathbf{R}) \mathbf{1} \Big] e^{i\omega R/c}, \quad (\text{B3})$$

where $\mathbf{R} = \mathbf{r} - \mathbf{r}'$. Note that the imaginary part of the free-space Green function is non-singular for $\mathbf{r} \rightarrow \mathbf{r}'$,

$$\lim_{\mathbf{r} \rightarrow \mathbf{r}'} \text{Im}[\mathcal{E}^{(0)}(\mathbf{r}, \mathbf{r}', \omega)] = \lim_{\mathbf{r} \rightarrow \mathbf{r}'} \text{Im}[\mathcal{H}^{(0)}(\mathbf{r}, \mathbf{r}', \omega)] = \frac{2\omega^3}{3c^3} \mathbf{1}. \quad (\text{B4})$$

In the limit $\mathbf{r} \rightarrow \mathbf{r}'$, the scattering part of the Green tensor $\mathcal{E}_{ij}^{(\text{sc})}(\mathbf{r}, \mathbf{r}', \omega)$ attains a finite limit, and its non vanishing components are

$$\begin{aligned} \mathcal{E}_{yy}^{(\text{sc})}(\mathbf{r}, \mathbf{r}, \omega) &= \mathcal{E}_{zz}^{(\text{sc})}(\mathbf{r}, \mathbf{r}, \omega) = 4\pi i \int \frac{d^2 \mathbf{k}_\perp}{(2\pi)^2} k_x \\ &\times \left[\left(\frac{R_p^{(1)} R_p^{(2)}}{\mathcal{A}_p} + \frac{\omega^2}{c^2 k_x^2} \frac{R_s^{(1)} R_s^{(2)}}{\mathcal{A}_s} \right) e^{2ik_x a} + \frac{1}{2} \left(\frac{\omega^2}{c^2 k_x^2} \frac{R_s^{(1)}}{\mathcal{A}_s} \right. \right. \\ &\left. \left. - \frac{R_p^{(1)}}{\mathcal{A}_p} \right) e^{2ik_x x} + \frac{1}{2} \left(\frac{\omega^2}{c^2 k_x^2} \frac{R_s^{(2)}}{\mathcal{A}_s} - \frac{R_p^{(2)}}{\mathcal{A}_p} \right) e^{2ik_x(a-x)} \right], \end{aligned} \quad (\text{B5})$$

and

$$\begin{aligned} \mathcal{E}_{xx}^{(\text{sc})}(\mathbf{r}, \mathbf{r}, \omega) &= 4\pi i \int \frac{d^2 \mathbf{k}_\perp}{(2\pi)^2} \frac{k_x^2}{k_x} \left(\frac{R_p^{(1)} R_p^{(2)}}{\mathcal{A}_p} e^{2ik_x a} \right. \\ &\left. + \frac{R_p^{(1)}}{2\mathcal{A}_p} e^{2ik_x x} + \frac{R_p^{(2)}}{2\mathcal{A}_p} e^{2ik_x(a-x)} \right), \end{aligned} \quad (\text{B6})$$

where \mathbf{k}_\perp is the in-plane wave-vector, $k_x = \sqrt{\omega^2/c^2 - k_\perp^2}$, the indices s and p denote TE and TM polarizations, respectively, $R_\alpha^{(k)}$ is the reflection coefficient of the k -th mirror for polarization $\alpha = s, p$ and $\mathcal{A}_\alpha = 1 - R_\alpha^{(1)} R_\alpha^{(2)} e^{2ik_x a}$. The corresponding formulae for the magnetic Green tensor $\mathcal{H}_{ij}^{(\text{sc})}(\mathbf{r}, \mathbf{r}, \omega)$ can be obtained from those of the electric Green tensor, by interchanging the reflection coefficients $R_s^{(k)} \leftrightarrow R_p^{(k)}$ into Eqs. (B5) and (B6).

As shown in Fig. 2, our mirrors consist of a metallic layer of thickness w , deposited on a thick Si substrate. The reflection coefficient R_α of a layered mirror with such a structure has the expression

$$R_\alpha(\omega, k_\perp; w) = \frac{r_\alpha^{(0 \text{ met})} + e^{2i w k_x^{(\text{met})}} r_\alpha^{(\text{met Si})}}{1 + e^{2i w k_x^{(\text{met})}} r_\alpha^{(0 \text{ met})} r_\alpha^{(\text{met Si})}}. \quad (\text{B7})$$

Here $r_\alpha^{(ab)}$ are the Fresnel reflection coefficients for a planar dielectric (we set $\mu = 1$ for all materials) interface separating medium a from medium b,

$$r_{\text{TE}}^{(ab)} = \frac{k_x^{(a)} - k_x^{(b)}}{k_x^{(a)} + k_x^{(b)}}, \quad (\text{B8})$$

$$r_{\text{TM}}^{(ab)} = \frac{\epsilon_b(\omega) k_x^{(a)} - \epsilon_a(\omega) k_x^{(b)}}{\epsilon_b(\omega) k_x^{(a)} + \epsilon_a(\omega) k_x^{(b)}}, \quad (\text{B9})$$

where $k_x^{(a)} = \sqrt{\epsilon_a(\omega) \omega^2/c^2 - k_\perp^2}$, and $\epsilon_a(\omega)$ is the complex frequency-dependent permittivity of medium a .

-
- [1] F. C. Auluck and D. S. Kothari, Proc. Roy. Soc. London, Ser. A **214**, 127 (1952).
 - [2] G. Barton, Phys. Rev. A **5**, 468 (1972).
 - [3] P. L. Knight, J. Phys. A **5**, 417 (1972).
 - [4] J. W. Farley and W. H. Wing, Phys. Rev. A **23**, 2397 (1981).
 - [5] J. M. Wylie and J. E. Sipe, Phys. Rev. A **30**, 1185 (1984).
 - [6] S. Haroche and D. Kleppner, Phys. Today **42**, 24 (1989).
 - [7] S. Y. Buhmann, *Dispersion Forces I: Macroscopic Quantum Electrodynamics and Ground-State Casimir, Casimir-Polder, and van der Waals Forces* (Springer, Berlin, 2012).
 - [8] L. Hollberg and J. L. Hall, Phys. Rev. Lett. **53**, 230 (1984).
 - [9] M. Marrocco, M. Weidinger, R. T. Sang, and H. Walther, Phys. Rev. Lett. **81**, 5784 (1998).
 - [10] V. Sandoghdar, C. I. Sukenik, E. A. Hinds, and S. Haroche, Phys. Rev. Lett. **68**, 3432 (1992).
 - [11] G. Bimonte, Phys. Rev. A **100**, 032501 (2019).
 - [12] H. Haakh, F. Intravaia, C. Henkel, S. Spagnolo, R. Pasante, B. Power, and F. Sols, Phys. Rev. A **80**, 062905 (2009).
 - [13] S. Y. Buhmann and S. Scheel, Phys. Rev. Lett. **100**, 253201 (2008).
 - [14] G. Barton, J. Phys. B **20**, 879 (1987).
 - [15] A. Corney, *Atomic and Laser Spectroscopy* (Clarendon Press, Oxford, 1977).
 - [16] K. Gottfried and T.-M. Yan, *Quantum Mechanics: Fundamentals* (Springer-Verlag, New York, 2003).
 - [17] S. G. Karshenboim, *Precision Physics of Simple Atomic Systems*, Ed. by S. G. Karshenboim and V. B. Smirnov (Springer, Berlin, Heidelberg, 2003), pp. 141-162.
 - [18] K. D. Bonin and V. V. Kresin, *Electric-Dipole Polarizabilities of Atoms, Molecules and Clusters* (World Scientific, Singapore, 1997).
 - [19] M.-P. Gorza and M. Ducloy, Eur. Phys. J. D **40**, 343 (2006).
 - [20] E. M. Lifshitz, Zh. Eksp. Teor. Fiz. **29**, 94 (1955) [Sov. Phys. JETP **2**, 73 (1956)].
 - [21] G. Bimonte, G. L. Klimchitskaya, and V. M. Mostepanenko, Phys. Rev. A **79**, 042906 (2009).
 - [22] N. F. Ramsey, *Molecular Beams* (Oxford Clarendon Press, UK, 1956).
 - [23] C. Kittel, *Introduction to Solid State Physics*, (Wiley, New York, 2005).
 - [24] N. W. Ashcroft and N. D. Mermin, *Solid State Physics* (Saunders College, Philadelphia, 1976).
 - [25] M. A. Ordal, R. J. Bell, R. W. Alexander Jr., L. L. Long,

- and M. R. Querry, Appl. Opt. **24**, 4493 (1985).
- [26] A. Messiah, *Quantum Mechanics* (Dover Publications, New York, 1995).
- [27] H. Bethe and E. Salpeter, *Quantum Mechanics of One- and Two-Electron Atoms* (Springer, Berlin, 1956).
- [28] The Fourier transform $f(\omega)$ of a function $g(t)$ is defined such that $f(\omega) = \int_{-\infty}^{\infty} dt g(t)$
- [29] Our normalization coincides with the k -scale of [27]